Dissimilar resistance spot welding of AISI 1075 eutectoid steel to AISI 201 stainless steel

Mehdi Safari [1*], Hossein Mostaan[2]

[1]*Department of Mechanical Engineering, Arak University of Technology, Arak 38181-41167, Iran*
[2]*Department of Materials and metallurgical Engineering, Arak University, Iran*

ARTICLE INFO

Article history:

Received 28 September 2016
Accepted 3 January 2016
Available online 15 March 2017

Keywords:

Dissimilar resistance spot welding
AISI 1075 eutectoid steel
AISI 201 stainless steel
Response surface methodology
Tensile-shear strength

ABSTRACT

In this paper, dissimilar resistance spot welding of AISI 1075 eutectoid steel to AISI 201 stainless steel is investigated experimentally. For this purpose, the experiments are designed using response surface methodology and based on four-factor, five-level central composite design. The effects of process parameters such as welding current, welding time, cooling time and electrode force are investigated on the tensile-shear strength of resistance spot welds. The results show that tensile-shear strength of spot welds increases with the increase in the welding current and welding time. Also, it is concluded that with increasing the electrode force and the cooling time, tensile-shear strength of the welded joints will decrease. During tensile-shear tests, three failure modes are observed, namely interfacial, partial pullout and pullout modes. The analysis of variance for the tensile-shear strength indicates that the main effects of welding current, electrode force, welding time, cooling time, second-order effect of the welding current and cooling time, two level interactions of welding current with welding time, welding current with cooling time and electrode force with cooling time are significant model terms. The results of analysis of variance (ANOVA) show that the presented model for tensile-shear strength of dissimilar resistance spot welds of AISI 1075 eutectoid steel to AISI 201 stainless steel can predict 95.00% of the experimental data and leave only 5.00% of the total variations as unexplained.

1-Introduction

Resistance spot welding (RSW) is the main joining process in automotive industry. This welding method is a low heat input process in which the heat is produced by the resistance of the parts being welded, as well as the interfaces, to the flow of localized current. The cooling rates of RSW are extremely high (in the order of 1000–10000 °C/s) [1]; therefore, it can be used as a suitable welding method for decreasing grain growth and preventing the formation of derogatory secondary phases which makes it a promising candidate for welding of steels. Automobile structural assemblies contain a few thousands of spot welds. Therefore, the quality, performance and the failure characteristics of resistance spot welds are important for determining the durability and safety design of the vehicles, as they transfer the load through the structure during a crash [2-4]. Like any other welding process, the quality of the joint in RSW is directly influenced by welding input parameters. A common problem faced by any manufacturer is the controlling of the process

* Corresponding author:
E-mail: *m.safari@arakut.ac.ir*, *ms_safari2005@yahoo.com*

input parameters to obtain a well welded joint with required strength. Thus, finding the relationships between the strength of spot weld and process parameters is of great interest in related industrial applications. Structures employing RSW joints are usually designed so that these joints are loaded in shear even if the parts are exposed to tension or compression loading. Therefore, the tensile–shear strength of spot weld is an important index to welding quality.

Static tensile shear test is the most common laboratory test used to determine the weld strength because of its simplicity. The majority of the research investigations in spot welding have been carried out on the joining of similar metals, particularly non-stainless steels. Engineers are increasingly encountering the need to join dissimilar materials as they are seeking creative new structures. Structures may need different properties like toughness or corrosion resistance in different areas. The total cost of the structure is another important consideration. To the authors' knowledge few documented data, guideline values and resistance weldability diagrams exist for RSW of dissimilar steels. There is also limited information available regarding the RSW of dissimilar metals like stainless steel and carbon steel. This study is carried out to determine the properties of resistance welded dissimilar metals at different welding parameters.

In recent years, some studies have been done on the dissimilar resistance spot welding process. Luo et al. [5] investigated the nugget formation of resistance spot welding (RSW) on dissimilar material sheets of aluminum and magnesium alloys. They analyzed microstructure and microhardness distribution near the joint interface. It was found that the staggered high regions at the contact interface of aluminum and magnesium alloy sheets, where the dissimilar metal melted together tended to be the preferred nucleation regions of nugget. Also, it was concluded that micro-cracks tended to generate at the interface of the nugget and base materials, which affected the weld quality and strength. Charde et al. [6] studied the material characterizations of mild steels, stainless steels, and both steel mixed joints under resistance spot welding process. Their results showed that stainless steels had higher tensile shear forces as compared to mild steel welds and mixed welds due to the natural hardness of the material. Also, the tensile shear forces of mixed welds had fluctuated between the mild and stainless steels shear forces. The mild and dissimilar steels micrographs had shown the fusion, heat-affected, heat-extended, and base metal zones very clearly, but heat-affected and heat-extended zones of the stainless steel were not visible at micro-level zooming because of the narrowed regions. Metallurgical views had clearly shown that the heat imbalance had occurred in mixed weld joints due to different electrical resistivity and thermal conductivity rates. Bina et al. [7] studied the effect of welding time on the joining capability of austenitic stainless steel (AISI 304) sheets and ferritic stainless steel (AISI 430) sheets by using resistance spot welding (RSW). They concluded that increase in the welding time resulted in an increase in the nugget size and the weld strength. Also, two distinct failure modes were observed during the tensile shear test: interfacial, pullout failure modes. Li et al. [8] investigated the effect of electromagnetic stirring upon the microstructure and mechanical properties of Al/Ti dissimilar materials resistance spot welding. In their work, the microstructures in the Al/Ti resistance spot weld joint were characterized by comparing them to those in an Al/Al resistance spot weld joint, and the effects of the welding current, welding time, and electrode force upon the tensile shear properties were also studied. Their results showed that under the action of EMS, a fine spheroidal grain structure formed in the Al/Ti joint and, compared with the traditional Al/Ti resistance spot weld, the weld created under the electromagnetic stirring effect exhibited a larger bonding diameter, and a higher tensile shear force and energy absorption. Zhang et al. [9] proposed a novel resistance spot welding method of dissimilar materials of 6008-T66 aluminum alloy and H220YD galvanized high strength steel. In their work, the morphology of welding electrodes was designed optimally. The optimized electrodes were a planar circular tip electrode with tip diameter of 10 mm on the steel side and a spherical tip electrode with spherical diameter of 70 mm on the aluminum alloy side. Their results showed that current density distribution during welding with optimized electrodes was more homogeneous

than that with F type electrodes. Furthermore, interfacial temperature in the welded joint during welding with optimized electrodes (about 915 °C) was lower than that welded with F type electrodes (about 985 °C). Min et al. [10] studied the dissimilar resistance spot welding of magnesium alloy AZ31B sheets and 443 ferritic stainless steel with cover plates under a relatively low welding current condition. In their investigations, metallurgical study of spot joints showed the cracks situated in only sideway of AZ31 weldment in the nugget under long welding time. Also, the tensile strength of the spot joint increases at first and decreases afterward. Zhang et al. [11] studied the dissimilar ultrasonic spot welding of aerospace aluminum alloy AA2139 to titanium alloy TiAl6V4. They investigated the microstructure, hardness, lap shear strength and fracture energy of spot welds. Their results showed that no obvious intermetallic reaction layer was observed in the AA2139–TiAl6V4 welds even by using transmission electron microscopy. Also, the hardness profile of AA2139 side after welding was studied, demonstrating that the heat introduced by the welding process leads to some softening with partial hardness recovery after natural aging. The effects of welding time on the peak load and fracture energy were investigated. The peak load and fracture energy of the welds increased with an increase in the welding time. Sun et al. [12] investigated the mechanical properties of dissimilar resistance spot welds of aluminum to magnesium with Sn-coated steel interlayer. Their results showed that the formation of Al–Mg intermetallic compounds was successfully prevented and strong Al/Mg resistance spot welded joints were achieved by inserting a Sn-coated steel interlayer between the two base metals before welding. The results showed that the thin Al–Fe reaction layer formed at the Al/steel interface did not significantly affect the tensile strength of the joints. Ighodaro et al. [13] studied the resistance spot welding of Al-Si coated and galvannealed (GA) hot stamping steels. Their results showed that the coating significantly affected the welding current required for attaining the conventionally acceptable weld fusion zone size. Also, they concluded that the coating influenced the energy absorption and failure mode transition but had no effect on the peak failure load provided that the stack consisted of sheets having similar coating.

Joining of dissimilar metals is of great importance in various applications. The most important application of joining between AISI 1075 and AISI 201 austenitic stainless steel is in automotive industries. To the authors' knowledge, no study has been devoted to the welding between these two metals. In this research, an attempt has been made to obtain a sound and defect-free weld between AISI 1075 and AISI 201 stainless steel. This goal has been obtained by a comprehensive study and through design and experiment. In this paper, dissimilar resistance spot welding of AISI 1075 eutectoid steel to AISI 201 stainless steel is studied experimentally. For this purpose, based on design of experiments and response surface methodology, the effects of process parameters such as welding current, welding time, cooling time and electrode force on the tensile-shear strength of dissimilar spot welds are investigated. The results obtained through response surface methodology are tested using analysis of variance (ANOVA). Based on the regression model, the optimum welding parameters can be identified, and that would provide valuable guidance for industrial applications of dissimilar resistance spot welding process of steels.

2- Design of Experiment

2-1- Response surface methodology

Response surface methodology (RSM) is a collection of mathematical and statistical techniques that are useful for modeling and analyzing engineering problems. Response surface methodology (RSM) proves to be effective in various applications for solving the multi-response optimization problems and it is considered one of the most common approaches to perform process optimization. In this technique, the main objective is to optimize (maximize or minimize or equal to a specific target value) the response surface that is influenced by various process parameters. Fundamental to RSM is the model that specifies the relationships among one or more measured responses and a number of accurately controllable predictors or input factors.

2-2- Experimental design

The experiment was designed based on four-factor, five-level central composite design. Welding current (6.4-14.4 KA), welding time (20-40 Cycles), cooling time (0-50 Cycles) and electrode force (800-2000 N) were the resistance spot welding input variables. In the present research each cycle is equal to $\frac{1}{50}$ second. In order to find the limitation of the process input parameters, trial weld runs were carried out by varying one of the process parameters at a time.

2-3- Experimental work

In the present work, AISI 1075 eutectoid steel and AISI 201 stainless steel with a thickness of 1 mm are used. Chemical compositions of both sheets are shown in Table 1. Also, mechanical properties of the base metals are presented in Table 2.

Table 1. Chemical composition (%) of the AISI 1075 eutectoid and AISI 201 stainless steel sheets.

	%C	%Si	%Mn	%P	%S	%Cr	%Ni
AISI 201	0.12	0.42	6.2	≤ 0.05	≤ 0.03	17.1	4.7
AISI 1075	0.74	0.18	0.75	≤ 0.012	≤ 0.005	0.40	0.3

Table 2. Mechanical properties of the AISI 1075 eutectoid and AISI 201 stainless steel sheets.

Base metal	Tensile Strength (MPa)	Yield Strength (MPa)	Elongation (%)	Young Modulus (GPa)	Hardness (Vickers)
AISI 1075	650	505	10	200	680
AISI 201	758	379	8	197	349

The resistance spot welded joints were produced using a constant alternating current resistance welder (Messer Griesheim) with a 150 kVA capacity, with its full digital setup parameter controlled by a microcomputer and pneumatic application mechanism. The welding was carried out by using water cooled conical electrodes having

a contact surface of the same diameter. In order to examine the mechanical properties of the joints, the tensile shear test was performed under a cross-head speed of 1.0 $mm.min^{-1}$ at room temperature. Tensile-shear test of the spot welded joints was done on a Kpruf universal testing machine. The welded parts according to ISO 14273 were prepared for tensile shear tests. The values of the tensile shear load were obtained from the load-extension graphs. Based on the design matrix (Table 3), experiments were conducted for 31 test samples. The results of the experiments are listed in Table 4.

Table 3. Actual values of the parameters for the RSW investigations.

Parameter	Units	Symbols	Limits				
Welding current	(kA)	I	6.4	8.4	10.4	12.4	14.4
Welding cycle	(cycle)	WC	20	25	30	35	40
Cooling cycle	(cycle)	CC	0	12.5	25	37.5	50
Electrode force	(N)	EF	800	1100	1400	1700	2000

Table 4. Design matrix with actual factors and measured mean responses.

Sample	Welding current (KA)	Electrode force (N)	Welding cycle	Cooling cycle	Tensile-Shear strength (N)
1	8.4	1100	25	12.5	4300
2	12.4	1100	25	12.5	6200
3	8.4	1700	25	12.5	4659
4	12.4	1700	25	12.5	6000
5	8.4	1100	35	12.5	4800
6	12.4	1100	35	12.5	6800
7	8.4	1700	35	12.5	4800
8	12.4	1700	35	12.5	6100
9	8.4	1100	25	37.5	4200
10	12.4	1100	25	37.5	5280
11	8.4	1700	25	37.5	3400
12	12.4	1700	25	37.5	4800
13	8.4	1100	35	37.5	5000
14	12.4	1100	35	37.5	6400
15	8.4	1700	35	37.5	5400
16	12.4	1700	35	37.5	6800
17	6.4	1400	30	25.0	3000
18	14.4	1400	30	25.0	6000
19	10.4	800	30	25.0	6000
20	10.4	2000	30	25.0	5000
21	10.4	1400	20	25.0	4500
22	10.4	1400	40	25.0	6000
23	10.4	1400	30	0.00	5400
24	10.4	1400	30	50.0	4900
25	10.4	1400	30	25.0	5700
26	10.4	1400	30	25.0	5710
27	10.4	1400	30	25.0	5690
28	10.4	1400	30	25.0	5680
29	10.4	1400	30	25.0	5740
30	10.4	1400	30	25.0	5720
31	10.4	1400	30	25.0	5760

Fig.1. Resistance spot welded specimens according to table 4 experiments.

In Fig.1 resistance spot welded specimens according to Table 4 experiments are shown. During tensile-shear test, three failure modes were observed, namely interfacial, partial pullout and pullout modes. Some spot welds with these three failure modes are shown in Fig.2.

a b c

Fig. 2. Three failure modes occurred during tensile shear tests; a- Interfacial mode in minimum tensile-shear strength, b- Partial pullout mode in middle tensile-shear strength, c- pullout mode in maximum tensile-shear strength

In Fig.3, three samples of calculated load-distance diagrams in the tensile test are shown. These load-displacement diagrams have been obtained for the resistance spot welded joints with maximum, middle, and minimum tensile-shear strengths.

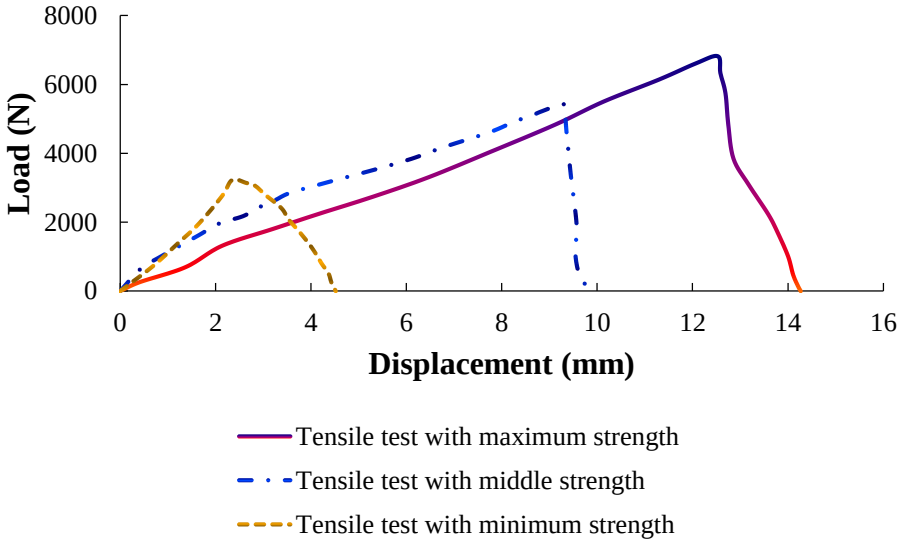

Fig.3. Load-displacement diagrams for the resistance spot welded joints with maximum, middle and minimum tensile-shear strengths.

3- Results and discussion

3-1- Analysis of variance (ANOVA)

The results of analysis of variance (ANOVA) for the tensile-shear strength are presented in Table 5. The adequacy of the developed model was tested using the ANOVA. The test for significance of the regression models, the F-test for significance on individual model coefficients and the lack-of-fit test were all performed using the same statistical package. Then, the step-wise regression method was used to eliminate the insignificant model terms automatically. So, the resulting ANOVA Table 6 for the model summarizes the analysis of variance for each response and shows the significant model terms. This table also shows the other adequacy measures R^2, adjusted R^2 and predicted R^2. They are all very close to 1, and therefore they indicate an adequate model. In fact, there is an adequate precision in the comparison of the range of the predicted value at the design points to the average prediction error.

Table 5. ANOVA results for tensile-shear strength value.

Term	Coef	SE Coef	T	P
Constant	5701.43	102.32	55.720	0.000
I	742.54	55.26	13.437	0.000
EF	-125.87	55.26	-2.278	0.037
WT	427.54	55.26	7.737	0.000
CT	-140.79	55.26	-2.548	0.022
I^2	-265.58	50.63	-5.246	0.000
EF^2	-15.58	50.63	-0.308	0.762
WT^2	-78.08	50.63	-1.542	0.143
CT^2	-103.08	50.63	-2.236	0.049
I×EF	-58.69	67.68	-0.867	0.399
I×WT	423.69	67.68	6.350	0.000
I×CT	-178.81	67.68	-3.164	0.001
EF×WT	76.31	67.68	1.128	0.276
EF×CT	286.19	67.68	4.228	0.001
WT×CT	3.81	67.68	0.056	0.956

Table 6. ANOVA test results for checking the adequacy of the proposed model.

Source	DF	Seq SS	Adj SS	Adj MS	F	P	Significance
Regression	14	22291423	22291423	1592245	21.72	0.000	OK
Linear	4	18475843	18475843	4618961	63.02	0.000	OK
Square	4	2248249	2248249	562062	7.67	0.001	OK
Interaction	6	1567330	1567330	261222	3.56	0.020	OK
Residual error	16	1172654	1172654	73291			
Lack-of-Fit	10	1169169	1169169	116917	201.25	0.000	OK
Pure Error	6	3486	3486	581			
Total	30	23464078					
R^2 = 95.00%							
Pred R^2 = 71.28%							
Adj R^2 = 90.63%							

SS: Sum of Square.
MS: Mean Square.
DF: Degree of Freedom.

As can be seen in Table 5, the analysis of variance for the tensile-shear strength indicates that the main effects of welding current (I), electrode force (EF), welding time (WT) and cooling time (CT) are significant model terms. Also, the second-order effects of the welding current (I^2) and cooling time (CT^2) are significant model terms. In addition, the two level interactions of welding current and welding time, welding current and cooling time, electrode force and cooling time are significant model terms.

It is concluded from Table 6 that the results of the ANOVA showed that the regression is significant with linear, quadratic, and interaction terms for the developed model. Regression odelling was performed to develop response equations with respect to input variables. Prior to regression modelling the input and output variables of the model were identified. Equation (1) presents the relationship between the process parameters and tensile-shear strength obtained by multiple linear regression analyses.

$$Tensile-shear\ strength = 5701.43 + 742.54 \times I - 125.87 \times EF + 427.54 \times WT - 140.79 \times CT - 265.58 \times I^2 - 103.08 \times CT^2 + 423.69(I \times WT) - 178.81(I \times CT) + 286.19(EF \times CT) \quad (1)$$

The validity of the model was checked by residual plots for tensile-shear strength as shown in Fig. 4. The normal probability plot of the residuals for tensile-shear strength, as shown in this figure, reveals that the residuals are falling on the straight line, indicating that the errors are distributed normally. The coefficient of determination "R^2" is used to find how close the predicted and experimental values lie. For a theoretically perfect statistical model, the value of R^2 is 1. This coefficient of determination (R^2) was calculated to be 0.9500 for the response of tensile-shear strength which indicates that the model can predict 95.00% of the experimental data and leave only 5.00% of the total variations as unexplained. All of the above considerations indicate the adequacy of the developed model.

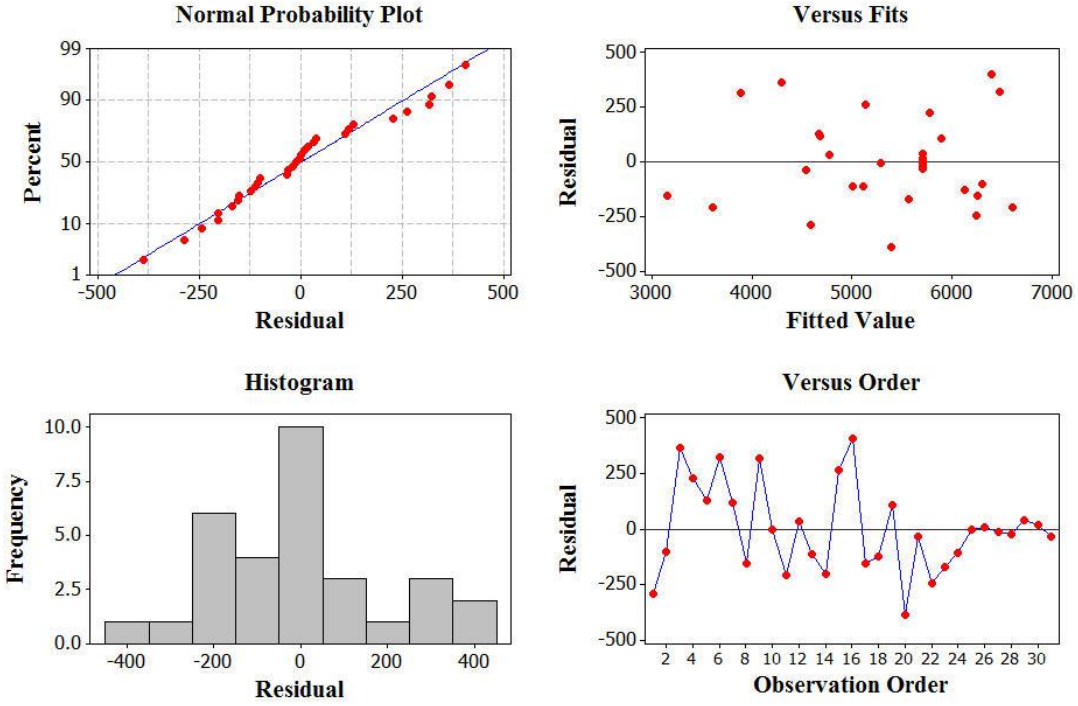

Fig.4. Normal probability plots for tensile-shear strength.

3-2- The effects of process parameters on the response

The main effects of different process variables on the tensile-shear strength, as predicted from the mathematical model are illustrated in Fig. 5. In general, the results show some convincing trends between the cause and the effect. According to the performed tests, we can conclude that the most effective RSW processing parameters are the welding current, the electrode force, the welding cycle and the cooling cycle. In the following, the effects of process parameters on the tensile-shear strength are explained.

As can be observed in Fig. 5, the tensile-shear strength of spot welds increases with increasing the welding current and welding time. This is because with increasing the welding current and also the welding time, generated heat in the welding area and also penetration depth will increase. Also, it is shown in Fig. 5 that with increasing the electrode force, the tensile-shear strength of welded joints will decrease. The reason is that when the electrode force increases the heat energy will decrease due to lower electrical resistance. It is concluded from Fig. 5 that the tensile shear strength of spot welded joints decreases with increasing the cooling time. The reason is that cooling time must not be too long as this may cause the heat in the weld spot to spread to the electrode and heat it.

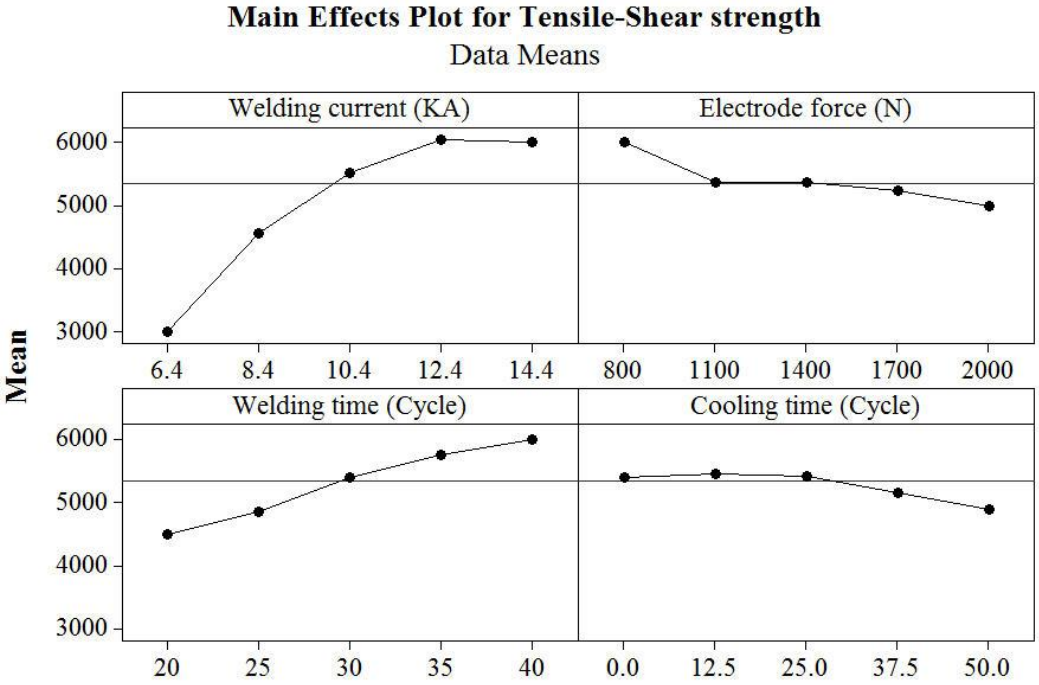

Fig.5. Plots of main effects on the tensile-shear strength.

3-3- Interaction effects of the process parameters

As it is presented in Table 5, the two level interactions of welding current and welding time, welding current and cooling time, electrode force and cooling time have significant effects on tensile-shear strength of resistance spot welds.

Fig. 6 demonstrates the interaction effect of welding current and welding time (electrode force is 1400 N and cooling time is 25 cycles).

As illustrated, within the range of 20–28 cycles for welding time, by increasing the welding current the strength increases within the range of 3000–6000 N. However, the welding time between 28-40 cycles leads to a sharp ascending rate in the tensile-shear strength and the strength of spot welds increases up to 6800 N. This happens due to the fact that more resistance heat is generated by increasing the welding current and time.

Fig. 7 demonstrates the interaction effect of the welding current and cooling time (electrode force is 1400 N and welding time is 30 cycles).

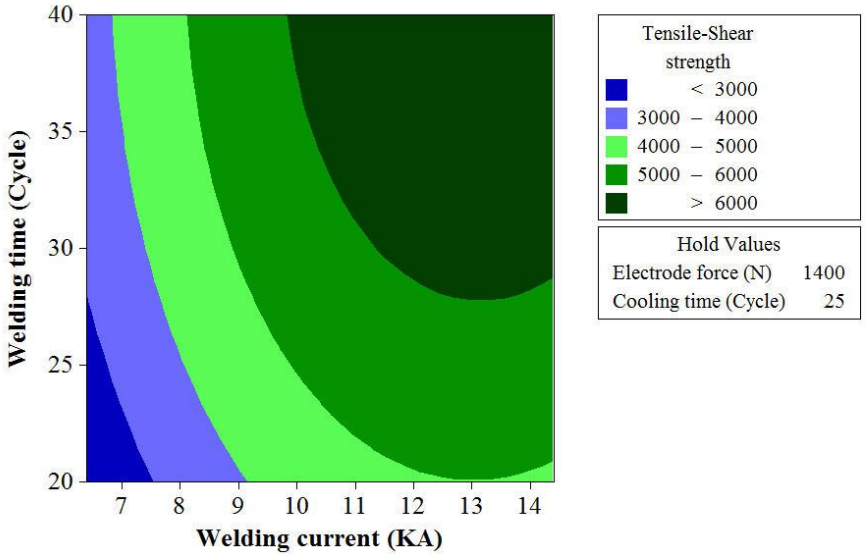

Fig.6. Contour plot of the interaction effects of welding current and welding time.

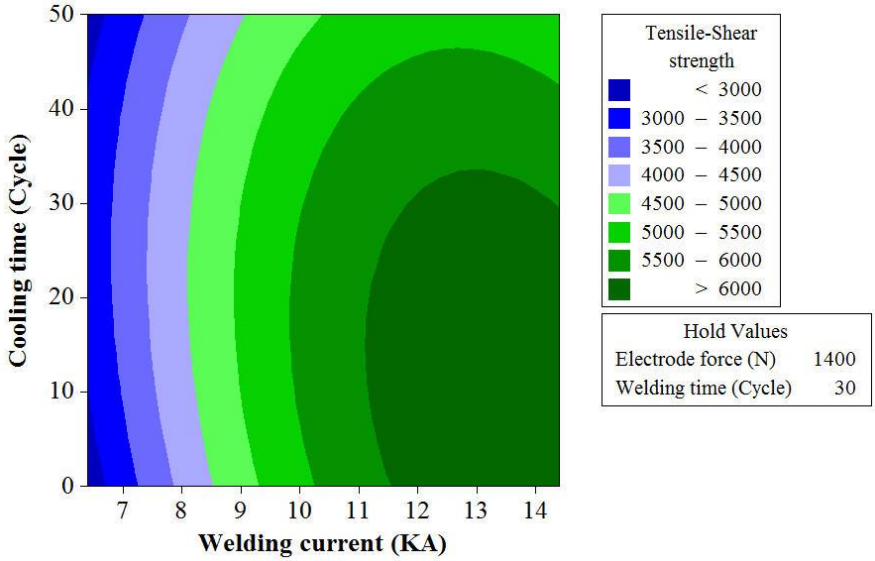

Fig.7. Contour plot of the interaction effects of welding current and cooling time.

As can be seen in Fig. 7, the tensile-shear strength of resistance spot welds increases with the increase in the welding current and decrease in the cooling time. It is concluded from Fig. 7 that in the low cooling cycles, welding current variations noticeably affect the tensile-shear strength in comparison with the effect of welding current on the tensile-shear strength at high cooling cycles. The reason is that cooling cycle must not be too long as this may cause the heat in the weld spot to spread to the electrode and heat it. The electrode will then get more exposed to wear. Fig. 8 gives the contour plot of the interaction effects of electrode force and cooling cycle, respectively.

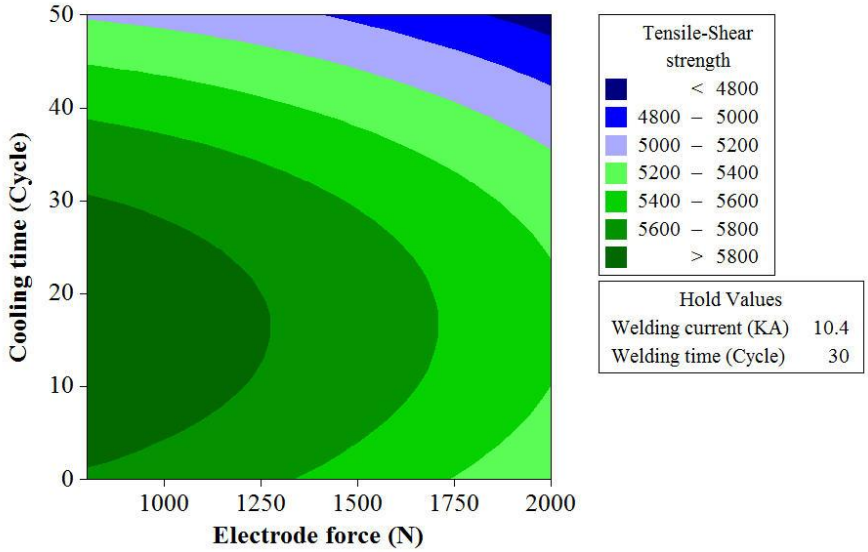

Fig.8. Contour plot of the interaction effects of electrode force and cooling time.

It is concluded from Fig. 8 that the tensile-shear strength of spot welds increases with decreasing the electrode force and cooling time. The reason is that when the electrode force is increased the heat energy will decrease due to lower electrical resistance. Also, when the electrode force is increased the heat energy will decrease. This means that the higher electrode force requires a higher weld current. When the weld current becomes too high, spatter will occur between electrodes and sheets. In other words, the weld metal sticks to the electrode face because of excessive heating of the metal sheet. Moreover, the weld metal spurts from between sheets resulting in a decrease in the tensile-shear strength. In addition, as it was mentioned above, the cooling cycle must not be too long as this may cause the heat in the weld spot to spread to the electrode and heat it.

The hardness profile from AISI 1075 eutectoid steel base metal to AISI 201 stainless steel base metal is shown in Fig. 9.

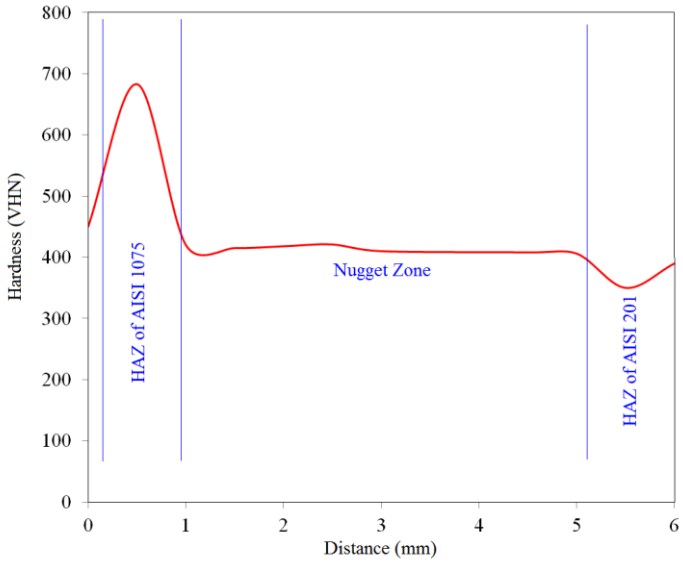

Fig. 9. The hardness profile from AISI 1075 eutectoid steel base metal to AISI 201 stainless steel base metal.

As can be seen in Fig. 9, the hardness value in the heat affected zone of AISI 1075 steel is higher than base metal. This increase in hardness value can be due to martensite phase formation in this area because of high hardenability of AISI 1075 steel. The hardness in the nugget zone is a medium value, while the hardness in the heat affected zone of AISI 201 is a minimum value. The decrease in the hardness value in this area is due to the austenite grain growth.

4- Conclusion

In this work, dissimilar resistance spot welding of AISI 1075 eutectoid steel to AISI 201 stainless steel was investigated experimentally. For this purpose, using design of experiments and based on response surface methodology and central composite algorithm, the effects of welding current, welding time, cooling time and electrode force on the tensile-shear strength of welded joints was examined. The following results were obtained in this paper:

1) During tensile-shear test, three failure modes were observed, namely interfacial, partial pullout and pullout modes.
2) Analysis of variance for the tensile-shear strength indicated that the main effects of welding current (I), electrode force (EF), welding time (WT) and cooling time (CT) were significant model terms. Also, the second-order effects of the welding current (I^2) and cooling time (CT^2) were significant model terms. In addition, the two level interactions of welding current and welding time, welding current and cooling time, electrode force and cooling time were significant model terms.
3) Analysis of variance showed that the regression was significant with linear, quadratic and interaction terms for the developed model. Also, for the presented model in this paper the coefficient of determination (R^2) was calculated to be 0.9500 for the response of tensile-shear strength which indicated that the model could predict 95.00% of the experimental data and leaved only 5.00% of the total variations as unexplained.
4) It was concluded that the tensile-shear strength of the spot welds increased with increasing the welding current and welding time. This is because with increasing the welding current and also the welding time, generated heat in the welding area and also penetration depth will increase.
5) It was shown that with increasing the electrode force, the tensile-shear strength of welded joints decreased. The reason is that when the electrode force is increased the heat energy will decrease due to lower electrical resistance. Also, when the electrode force increases the heat energy will decrease. This means that the higher electrode force requires a higher weld current. When weld current becomes too high, spatter will occur between electrodes and sheets. In other words, the weld metal sticks to the electrode face because of excessive heating of the metal sheet. Moreover, the weld metal spurts from between sheets resulting in a decrease in the tensile-shear strength.
6) It was proved that the tensile shear strength of spot welded joints decreased with increasing the cooling time. The reason is that cooling time must not be too long as this may cause the heat in the weld spot to spread to the electrode and heat it.

References

[1] W. L. Chuko, J. E. Gould, Development of appropriate resistance spot welding practice for transformation-hardened steels, Welding Journal, 1s–7s, 2002.

[2] X. Yuan, C. Li, J. Chen, X. Li, X. Liang, X. Pan, Resistance spot welding of dissimilar DP600 and DC54D steels, Journal of Materials Processing Technology, 239, (2017) 31–41.

[3] K. Chung, W. Noh, X. Yang, H. N. Han, M. G. Lee, Practical failure analysis of resistance spot welded advanced high-strength steel sheets, International Journal of Plasticity,

[4] J. Chen, X. Yuan, Zh. Hu, Ch. Sun, Y. Zhang, Y. Zhang, Microstructure and mechanical properties of resistance-spot-welded joints for

A5052 aluminum alloy and DP 600 steel, Materials Characterization, 120, (2016) 45-52.
[5] Y. Luo, J. Li, Analysis of Nugget Formation During Resistance Spot Welding on Dissimilar Metal Sheets of Aluminum and Magnesium Alloys, Metallurgical and Materials Transactions A, Vol. 45A, pp. 5107- 5113, 2014.
[6] N. Charde, F. Yusof, R. Rajkumar, Material characterizations of mild steels, stainless steels, and both steel mixed joints under resistance spot welding (2-mm sheets), International Journal of Advanced Manufacturing Technology, Vol. 75, pp. 373-384, 2014.
[7] M. H. Bina, M. Jamali, M. Shamanian, H. Sabet, Effect of welding time in the resistance spot welded dissimilar stainless steels, Trans Indian Inst Met (2015) 68(2):247–255.
[8] Y. Li, Y. Zhang, J. Bi, Z. Luo, Impact of electromagnetic stirring upon weld quality of Al/Ti dissimilar materials resistance spot welding, Materials & Design, Volume 83, 15 October 2015, Pages 577–586.
[9] W. Zhang, D. Sun, L. Han, Y. Li, Optimised design of electrode morphology for novel dissimilar resistance spot welding of aluminium alloy and galvanised high strength steel, Materials and Design 85 (2015) 461–470.
[10] D. Min, Zh. Yong, L. Jie, Dissimilar spot welding joints of AZ31-443 ferritic stainless steel with cover plate, International Journal of Advanced Manufacturing Technology, DOI: 10.1007/s00170-015-8078-y.
[11] C.Q. Zhang, J.D. Robson, P.B. Prangnell, Dissimilar ultrasonic spot welding of aerospace aluminum alloy AA2139 to titanium alloy TiAl6V4, Journal of Materials Processing Technology, 231 (2016), Pages 382–388.
[12] M. Sun, S.T. Niknejad, H.Gao, L.Wu, Y.Zhou, Mechanical properties of dissimilar resistance spot welds of aluminum to magnesium with Sn-coated steel interlayer, Materials and Design 91 (2016) 331–339.
[13] O.L. Ighodaro, E. Biro, Y.N. Zhou, Comparative effects of Al-Si and galvannealed coatings on the properties of resistance spot welded hot stamping steel joints, Journal of Materials Processing Technology, DOI: 10.1016/j.jmatprotec.2016.03.021.